The Egyptian Journal of Radiology and Nuclear Medicine (2015) **46**, 215–224

Egyptian Society of Radiology and Nuclear Medicine

The Egyptian Journal of Radiology and Nuclear Medicine

www.elsevier.com/locate/ejrnm
www.sciencedirect.com

ORIGINAL ARTICLE

Role of multiphasic multi-detector computed tomography (MDCT) in the diagnosis and staging of solid neoplastic renal masses

Manal H. Wahba [a,*], Tamer W. Kassem [a], Ahmed A.S. Mahmoud [b]

[a] *Radiology Department, Cairo University, Egypt*
[b] *Radiology Department, Tudor Bilharz Research Institute, Egypt*

Received 20 August 2014; accepted 20 September 2014
Available online 18 October 2014

KEYWORDS

Multiphasic MDCT scan;
Solid renal masses;
RCC

Abstract *Objectives:* The aim of this study was to assess the role of multi-detector computed tomography (MDCT) in diagnosis and preoperative staging of solid renal masses.
Patients and methods: During two years duration we prospectively evaluated 56 patients with solid renal lesions previously detected by US. All patients underwent multiphasic CT scanning for the kidneys and urinary tract following a preset scanning protocol that included unenhanced, corticomedullary phase (CMP), nephrograhic phase (NP) and excretory phase (EP) scanning. The images obtained in the excretory delayed phase were reconstructed in different planes to obtain 2D and 3D reformatted images providing volume rendering VR and maximum intensity projection (MIP) CTU images. Curved reformatting was sometimes used for the ureter. The numbers of lesions detected in all three phases were determined. Results of CT scan were compared with histopathology or constellation of clinical and imaging patient data.
Results: A total of 61 masses were detected in 56 cases, 51 cases had unilateral masses (91%), 5 cases had bilateral masses (**9**%). The different pathologies encountered in the study were RCC 39 masses (64%), Wilm's tumor 3 masses (4.9%), transitional cell carcinoma 3 masses (4.9%), angiomyolipoma 7 masses (11.5%), lymphoma 6 masses (9.8%), metastasis one mass (1.6%), angiomyolipoma associated with RCC two masses (3.3%). Lymph nodal metastasis, renal vein, IVC thrombosis and distant metastatic spread in different pathologies were assessed.
The attenuation HU values calculated in the early CMP for all cases of RCC had a mean value of 80.5 HU (STD 45.7) while the mean values in NP and EP were 70.6 HU (STD 25.4) and 51.3 HU (STD 19.2) respectively.
A pattern of enhancement was detected in all cases of RCC in the form of rapid wash out of contrast and decrease of attenuation (HU) by time throughout different phases.
Significant difference between HU in CMP and EP in cases of RCC (P value = 0.0002) and difference between HU in NP and EP in cases of RCC (P value < 0.00001) were found.

* Corresponding author.
Peer review under responsibility of Egyptian Society of Radiology and Nuclear Medicine.

http://dx.doi.org/10.1016/j.ejrnm.2014.09.004
0378-603X © 2014 The Egyptian Society of Radiology and Nuclear Medicine. Production and hosting by Elsevier B.V. All rights reserved.

Conclusion: Multiphase multislice computed tomography combined with CT angiography and CT urography have a major role in solid renal neoplastic masses' diagnosis, characterization and differentiating benign and malignant tumors.

© 2014 The Egyptian Society of Radiology and Nuclear Medicine. Production and hosting by Elsevier B.V. All rights reserved.

1. Introduction

Improvement in imaging modalities continues to have a large impact on the diagnosis and treatment of solid renal masses. As many as 30–40% of renal tumors are discovered incidentally during evaluation of unrelated or unspecific symptoms, and many lesions can be appropriately treated with local excision and maximal preservations of the surrounding unaffected parenchyma (1).

The advent of multi detector CT scan has enabled us to delineate the mass, detect and map the extent of venous spread, lymph nodal enlargement and diagnose local or distant spread. (2) Accordingly, differentiation between benign and malignant masses and accurate staging of malignant ones was obtained. Treatment regimen is then planned whether medical or surgical solutions (6).

The aim of this study was to assess the role of multidetector computed tomography (MDCT) in diagnosis and preoperative staging of solid renal masses.

2. Patients and methods

2.1. Patients

During two years duration fifty-six patients were prospectively included in this study. They were referred to the Radiology department in Cairo University Hospitals for further assessment of renal masses previously detected by US using mutliphase MDCT of the urinary system. These patients were 33 males and 23 females with their ages ranging between 3 and 75 years (mean 47.4 years, STD 17.43).

They were subjected to full clinical history and routine laboratory investigations as well.

2.2. Methods

All patients underwent multiphasic CT scanning following a preset scanning protocol that included unenhanced, corticomedullary phase (CMP), nephrograhic phase (NP) and excretory phase (EP) scanning.

The examination was performed using sixty-four section MDCT scanner (Aquillion, Toshiba Medical Systems, Japan). For acquisition of all images, a tube voltage of 140 kVp, a tube current of 200–300 mA, slice thickness of 1.25 mm, pitch of 1:1.5, speed 7.5 mm per rotation, gantry rotation 0.8 s were used.

In all patients, initial scanning was done before administration of contrast medium. The non enhanced phase was done at 5 mm thickness and speed 15 mm per rotation.

Patients then received 2 ml/kg body weight of low osmolar non-ionic contrast medium (Ultravist 300 mg/ml, Bayer) at the rate of 3.5–4 ml/s and 150 mmHg. The NP images were obtained with a delay of 50 s after initiation of contrast medium injection, scanning time about 30 s. The EP delay was obtained with 350–400 s delay and scanning time 60 s. In the precontrast scan and EP the area scanned was from the level of diaphragm to symphysis pubis. However in CMP and NP, scanning area was from the diaphragm to iliac crest.

2.3. Data analysis and interpretation

All images throughout different phases of the examination were sent to remote workstation (Vitrea Workstation). The images obtained in the early arterial phase were reconstructed in different planes to obtain 2D and 3D reformatted images providing VR and MIP CTA images.

The images obtained in the excretory delayed phase were reconstructed in different planes to obtain 2D and 3D reformatted images providing VR and MIP CTU images. Curved reformatting was used for the ureter.

After confirmation of the presence of solid renal mass, certain information was then fulfilled including their locations, extensions, relation to collecting system, peri-nephric spread, local infiltrations, venous involvement, renal vascular anatomy, regional lymph nodes and distant abdominal and lung bases metastasis.

Staging depends on the previously collected data. TNM score was used in cases of RCC.

A certain region of interest (ROI) was determined within the mass in condition not to include calcifications or areas of cystic degenerations which may result into false high or low attenuation values. We kept the sizes and locations of the regions of interest the same for each patient's images from the three scanning phases. The attenuation (HU) in each ROI was calculated automatically using DICOM image viewer. All values were collected and tabulated aiming to obtain certain pattern of enhancement for each group of pathology. The MSCT findings were correlated with the results of histopathological findings after surgery and follow up.

3. Results

A total of 61 solid renal masses were detected in 56 cases, 51 cases had unilateral masses (91%), 5 cases had bilateral masses (9%). These 5 cases with bilateral lesions include one case of bilateral angiomyolipoma, one case of bilateral renal cell carcinoma (Fig. 1) and 3 cases of bilateral lymphoma. The one case of bilateral angiomyolipoma was diagnosed as tuberous sclerosis after further investigations of other systems by different imaging modalities.

Out of 61 masses, 54 masses (88.5%) were malignant and 7 masses (11.5%) were benign. The different pathologies encountered in the study were renal cell carcinoma (RCC) 39 masses (64%), Wilm's tumor 3 masses (4.9%) (Fig. 2),

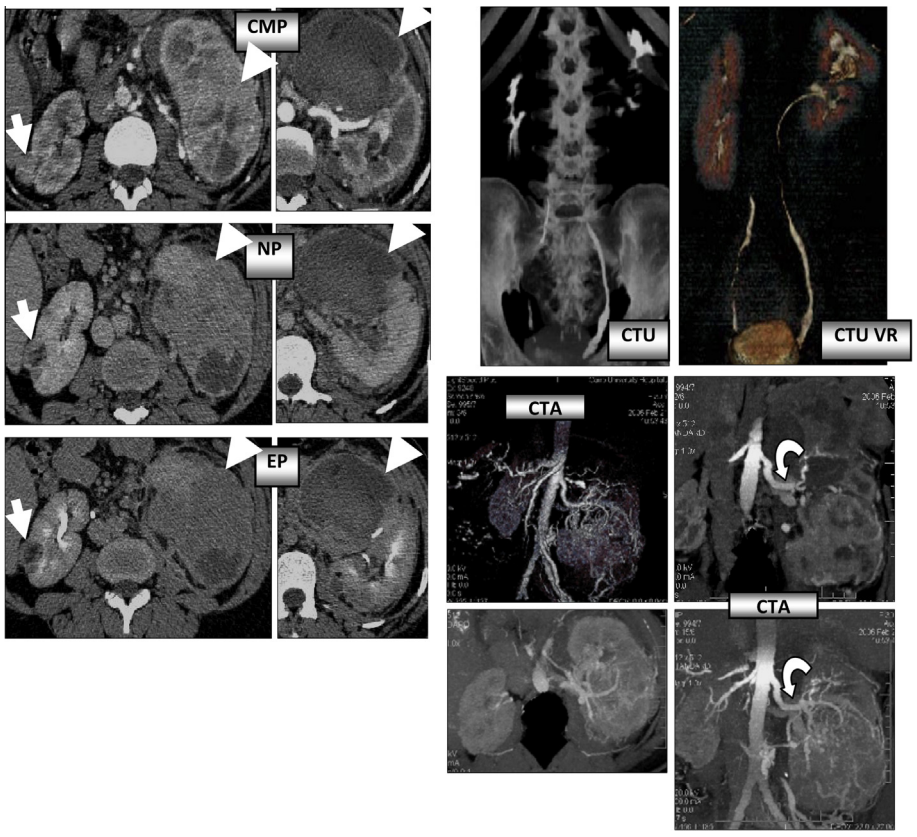

Fig. 1 30 year old patient presented with abdominal pain and hematuria. MDCT: Left kidney: Large well defined lower zonal soft tissue mass (arrow heads) showing heterogeneous texture and measuring >7 cm in diameter. It shows intense enhancement in the CMP and rapid wash out in the following NP (HU is 124.6 in CMP, 81.3 in NP and 61.6 in EP). The mass extends beyond the renal fascia with multiple linear streaky densities and minimal amount of fluid. Patent left renal vein and IVC. Another large predominantly cystic mass is also seen at the upper pole. Right kidney: Small rounded well defined cortical lower pole soft tissue mass lesion (arrows) measuring <4 cm in diameter with no evidence of local infiltration. Multiple variable sized enlarged abdominal lymph nodes are seen involving the para-aortic, celiac and superior mesenteric groups. CTA: Hypertrophied left main renal artery (curved arrows) and supplying segmental branches with early venous filling of the draining veins. CTU: Dilated left pelvicalyceal system with no evidence of invasion. The left ureter is seen displaced anteriorly and medially. Normal size and configuration of the right pelvicalyceal system. Diagnosis: Bilateral renal cell carcinoma, left (Sarcomatoid subtype) T4 N2 M1, right (Clear cell subtype).

transitional cell carcinoma 3 masses (4.9%), angiomyolipoma 7 masses (11.5%), lymphoma 6 masses (9.8%), metastasis one mass (1.6%), angiomyolipoma associated with RCC two masses (3.3%) as listed in Table 1.

The MSCT were correlated with the results of histopathology and follow up. Lymph nodal metastasis, renal vein, IVC thrombosis and distant metastatic spread in different pathologies were assessed. The CT diagnosis of lymph node metastases was reliant on nodal enlargement of greater than 1 cm in short-axis diameter.

Nine out of 39 RCC (23%) masses have shown lymph nodal metastasis while all Wilm's and lymphoma masses have shown nodal metastasis (100%).

Perinephric extension was detected in 16 renal masses. Eight out of 39 RCC (20.5%), in 2 out of 3 (66.6%) Wilm's tumors and in all six cases (100%) of lymphoma.

Four out of 39 RCC masses had distant metastatic spread (10%) (three cases with lung metastasis and one case with liver metastasis), two out of 3 Wilm's masses (66.6%) while all lymphoma and metastasis masses (100%) had distant abdominal metastatic spread as listed in Table 2.

Two out of seven cases of angiomyolipoma, demonstrated appreciable fat on CT images and the diagnosis was done based on CT findings (Fig. 3), they showed a stable course in 1 year follow up. While the remaining 5/7 cases (71%) showed absence of fat density which necessitates further surgical assessment and pathological diagnosis.

Among 39 masses of RCC, 2 cases had renal vein thrombosis with a percentage of 5%. These two cases showed thrombus extension to inferior vena cava (IVC).

Thirty-nine masses in 38 cases were subjected to TNM classification, 13 cases of RCC (34%) were staged as T1a due to small size of the mass (<4 cm). Ten cases of RCC (26%) had masses measuring 4–7 cm in diameters and staged as T1b. 7 cases of RCC (18.4%) staged as T2 had large masses (>7 cm in diameters).

Two out of 38 RCC cases (5%) showed extension to the peri renal fat and staged as T3a while one case (2.6%) staged as T3c had renal vein thrombosis extending to the IVC above the diaphragm (Fig. 4).

Local infiltration and extension of the neoplastic mass beyond the renal fascia were detected in 5/38 cases (14%)

Fig. 2 A 14 year old female patient presented with marked abdominal distension and contour bulge of the abdominal cavity. MDCT: Large soft tissue mass (arrow heads) occupying most of the abdominal cavity and crossing midline showing large ill defined cystic areas (asterisk). CTA: The right main renal artery is inconspicuous. Multiple arterial collaterals (arrows) are seen supplying the mass originating from the celiac trunk, superior and inferior mesenteric, common iliac and epigastric arteries. CTU: No evidence of contrast excretion by the right kidney. Diagnosis: Wilm's tumor, Stage III.

diagnosed as T4. One among these cases also had renal vein and IVC thrombosis extending to a level below the diaphragm.

Regional lymph nodal metastasis limited to one group of nodes was detected in 5 cases (10%) (N1) and in more than one group of lymph nodes in 4 cases (10%) (N2) Table 3, distant metastasis was detected in 4 cases (10.5%) with 2 cases showing liver metastases and 2 cases showing basal lung metastases.

Table 1 Different pathologies encountered in the study.

Pathology	No. of masses	%
RCC	39	64
Wilm's	3	4.9
TCC	3	4.9
AML	7	11.5
Lymphoma	6	9.8
Metastasis	1	1.6
AML/RCC	2	3.3
All	61	100

We measured the HU of TCC and RCC cases in CMP, NP and EP .The attenuation HU values calculated in the early CMP for all cases of RCC had a mean value of 80.5 HU (STD 45.7) while the mean values in NP and EP were 70.6 HU (STD 25.4) and 51.3 HU (STD 19.2) respectively.

A pattern of enhancement was detected in all cases of RCC in the form of rapid wash out of contrast and decrease of attenuation (HU) by time throughout different phases (Fig. 5).

Significant difference between HU in CMP and EP in cases of RCC (P value = 0.0002) and difference between HU in NP and EP in cases of RCC (P value < 0.00001) were found.

Pathologically proven cases of RCC clear cell subtype showed intense enhancement in the early CMP (HU 144.7 and 129.7) and rapid wash out of contrast in the following NP (HU 79.8 and 88.4) respectively. The pathologically proven case of papillary subtype showed minimal enhancement in the CMP (HU 55.5) and homogenous faint enhancement in the NP (HU 83.1) (Fig. 6).

39 RCC masses (regardless of their pathological subtypes) showed intense enhancement in the CMP (mean 80.5 HU, STD 45.7), rapid decrease of enhancement in the following NP (mean 70.6 HU, STD 25.4) denoting rapid wash out of contrast and final decrease of HU in the EP (mean 51.3 HU, STD 19.2). A significant difference was detected between HU in CMP and EP in cases of RCC (P value = 0.0002) and difference between HU in NP and EP in cases of RCC (P value < 0.00001).

TCC (3 cases) showed a faint enhancement in the CMP (mean 40.6 HU, STD 27.8), further increase of enhancement in the following NP (mean 59.4 HU, STD 8.7) and final decrease of HU in the EP (mean 37.1 HU, STD 19.8). A significant difference was detected between HU in NP and EP in cases of TCC (P value = 0.03).

4. Discussion

Improvement in imaging modalities continues to have a large impact on the diagnosis and treatment of solid renal masses. As many as 30–40% of renal tumors are discovered incidentally during evaluation of unrelated or unspecific symptoms. (1,18).

Multidetector spiral CT remains the single most effective imaging modality for the diagnosis and staging of renal cell carcinoma. In the majority of patients, it is the only imaging test needed prior to surgical management. Advances in data acquisition and display, including three-dimensional volume

Table 2 Showing lymph nodal metastasis and perinephric extension and distant metastatic spread detected, the CT diagnosis of lymph node metastases is reliant on nodal enlargement of greater than 1 cm in short-axis diameter.

Pathology	LNs		Perinephric extension		Distant metastasis	
	No	%	No	%	No	%
RCC	9/39	23	8/39	20.5	4/39	10
Wilm's	3/3	100	2/3	66.6	2/3	66.6
TCC	0/3	0	0/3	0	0/3	0
Lymphoma	6/6	100	6/6	100	6/6	100
Metastasis	–	–	–	–	1/1	100

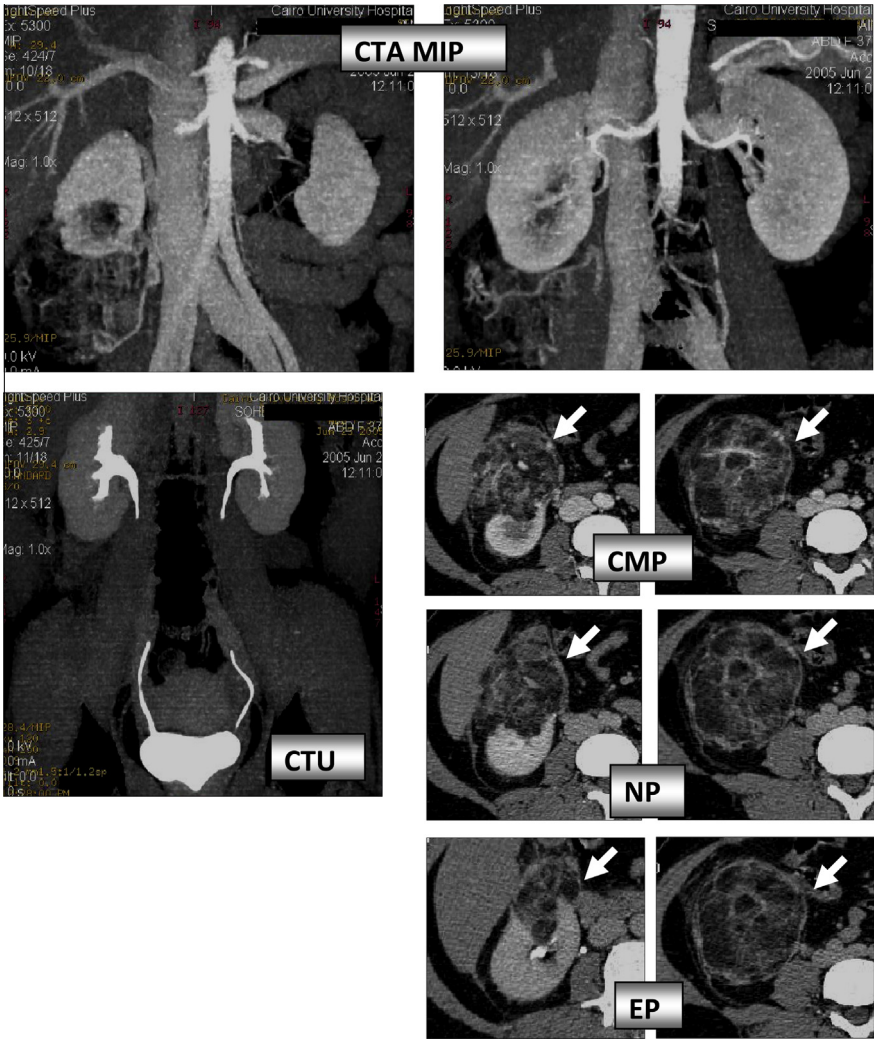

Fig. 3 MDCT: Large right renal lower pole cortical soft tissue mass showing heterogeneous texture, areas of intense enhancement and areas of fat densities (arrows). CTA: No pathological circulation. Multiple dilated and tortuous vascular channels with early venous filling of the hypertrophied draining veins. CTU: No abnormality detected. Diagnosis: Angiomyolipoma.

rendering techniques, provide unparalleled capabilities for the detection, staging, and management of primary renal cell carcinoma (2,8).

Treatment decisions hinge on the extent and stage of the tumor. Since the only curative treatment for renal cell carcinoma remains complete surgical excision, the goals of preoperative CT are to delineate the primary tumor, detect and map the extent of venous spread, and diagnose local or distant metastases (12).

Dedicated renal CT performed for the diagnosis and staging of renal solid neoplasm must include a combination of image data acquisitions, despite the added radiation exposure and cost. Better detection and characterization of renal masses, as well as more accurate staging, are possible when the

Fig. 4 A 57 year old male patient presented with continuous right hypochondrial pain, recurrent attacks of hematuria, and rapid loss of weight. MDCT: The right kidney is almost totally replaced by a large soft tissue mass, sparing the upper pole with heterogeneous texture, intense enhancement in the CMP and rapid wash out of contrast in the following NP and become hypodense the EP. The mass extends beyond the perirenal fascia. Right adrenal deposit (black arrow). Multiple variable sized hepatic deposits (white arrows). Multiple enlarged abdominal and pelvic lymph nodes. The renal vein and IVC are distended and totally occluded by tumoral thrombus (arrow heads). The thrombus extends caudally till CIV and cranially crossing above the diaphragm and reaching the right atrium (curved arrows). Diagnosis RCC T4 N2 M1.

scanning protocol includes a combination of unenhanced CT and imaging in the corticomedullary and nephrographic phases (4,13).

In this study we assessed the role of MSCT for the diagnosis and preoperative staging of solid renal lesions. Fifty six patients with 61 renal masses were prospectively evaluated using MSCT in different phases. MSCT was useful for characterization of renal lesions, as it failed to diagnose only 5 cases of AML due to absence of characteristic fat density. The non fat containing angiomyolipoma accounts for 8.9% in our study with diagnostic accuracy of the MSCT reaching 91%, consistent with the study of Zhang et al. (17).

In this study we performed CT staging for malignant renal lesions. We found that most of RCC lesions (33 cases, 54.5%) were early stage; (8 cases T1a, 24.2% and 10 cases T1b, 3.0%). This is consistent with the downward migration in the size and

Table 3 TNM staging in 38 RCC cases.

Stage	No. of cases with RCC	Percent
T1a	13	34
T1b	10	26
T2	7	18.4
T3a	2	5
T3c	1	2.6
T4	5	14
N0	29	77
N1	5	14
N2	4	10
M0	34	92
M1	4	10.5

stage of renal cortical tumors at presentation that has occurred over the last decade. Despite the generally small sizes of these lesions, their characterization based on imaging features and degree of enhancement could be achieved. That is in agreement with the study of (17) that reported most of the patients had early-stage tumors at the time of presentation (T1a, 62%; T1b, 12%; T2, 8%; T3, 13%; and T4, < 1%).

The rest of our RCC cases had more advanced stages as 7 cases were staged T2 (21.2%), 2 cases T3a (6%), 1 case T3b (3%) and 5 cases T4 (15.1%) with a total of 15 cases representing 45.4% of RCC cases. These results demonstrate that our patient population had renal cell carcinomas of relative delayed stages compared to other studies as those of (18).

The evaluation of renal vein thrombosis is crucial for treatment planning; in fact, if tumor thrombus spreads into the inferior vena cava, the exact extent of the thrombus is essential for planning the correct surgical approach: an abdominal incision is performed if the thrombus is infra hepatic, whereas a thoraco-abdominal incision is needed if the thrombus extends more cranially (1). Two patients in this study with the diagnosis of RCC had renal vein and IVC invasion (6%) staged as T3c and T4. One case had supra diaphragmatic extension till the right atrium.

Ng et al. and Sheth et al.(2,12) reported that extension of renal cell carcinoma into the renal vein alone (stage T3b) occurs in approximately 23% of patients and does not adversely affect the prognosis. Spread of the tumor into the IVC is found in 4–10% of patients (14).

Our result goes with Staehler and Brkovic (14) regarding IVC thrombosis while percentage of renal vein thrombosis in our study is lower than Sheth et al. (12) possibly due to smaller number of patients in our study and majority of cases in early stages (54.5% of RCC T1a and T1b).

Involvement of the perirenal fat tissue represents a key point in treatment planning. In fact, the infiltration of the perirenal fat tissue modifies the surgical approach from conservative to radical nephrectomy (15).

Under and over staging of perinephric invasion are the most common staging errors at CT. The most specific finding of stage T3a disease, is the presence of an enhancing nodule in the perinephric space. (12). Tumor mis-staging after MDCT is of little clinical importance, however in our study large tumor size > 7 cm (18.4%) is a risk factor for tumor mis-staging and this is in line with that stated in (3).

In our study, out of 54 malignant masses, perinephric extension was seen in 16 renal masses, eight out of 39 RCC, 2 out of 3 Wilm's tumors and all 6 cases of lymphoma. Local infiltration and extension of the neoplastic mass beyond the renal fascia were detected in 5 cases (14%) diagnosed as T4. One among these cases had also renal vein and IVC thrombosis extending to a level below the diaphragm.

Despite its complexity, the TNM classification, which defines the anatomic extent of the tumor more precisely, has gained wide acceptance (10).

Regarding lymph nodal metastasis our study included 29 cases of RCC (72.7%) that had not been associated with lymph nodal enlargement N0. However Sheth et al. (12) stated that in more than half of the patients in their study, nodal enlargement was caused by benign inflammatory changes. Nodal enlargement shown at CT should not disqualify patients from nephrectomy unless metastatic spread is confirmed with fine-needle aspiration.

Among all renal cortical tumors detected, approximately 20% are benign lesions and 25% are relatively indolent papillary or chromophobe carcinomas. It appears that although 80% of renal cortical tumors are malignant, not all malignant tumors undergo substantial active growth. Without tumor growth, the risk of metastasis may be limited as well. Thus, treatment strategy may differ according to the patient's age, general medical condition, and renal function status, as well as the aggressiveness of the detected renal tumor. Since different subtypes of renal tumors are associated with different clinical implications, it is clinically important to differentiate these lesions preoperatively (16,17).

The results of previous studies reported that certain imaging features may be associated with specific subtypes of renal cortical tumor. The degree of enhancement was the most valuable parameter for differentiation of RCC subtypes, as clear cell RCCs enhance to a greater degree than other subtypes of malignant lesions, especially papillary RCCs (5–7,9,11).

In addition, Herts et al. (5) previously found that papillary RCCs are typically homogeneous and hypovascular on CT and angiography. They also found that high attenuation in tumors on CT correlates with clear cell carcinomas. Most of these studies included only malignant lesions or, in some cases, subgroups of malignant lesions in their analyses.

In our study we included solid renal masses of different etiologies: both malignant and benign tumors, while our patient cohort was relatively small (total of 61 renal masses and 39 masses of RCC).

In our study, there was one case of papillary subtype of RCC which showed minimal enhancement in the CMP (HU 55.5) and homogenous faint enhancement in the NP (HU 83.1), compared to the enhancement pattern of RCC clear cell subtype which showed intense enhancement in the early CMP (HU 144.7 and 129.7) and rapid wash out of contrast in the following NP (HU 79.8 and 88.4) respectively.

In this study we measured the HU of RCC lesions in different phases of contrast injection. Since renal tumors are often heterogeneous, we decided to measure areas of greatest enhancement in the lesion rather than in the entire tumor. This minimizes volume averaging effects from areas of cystic or necrotic changes and truly reflects the vascularity of the tumor. Because of the small size and heterogeneous nature of many renal lesions, the selection of areas of greatest degree of

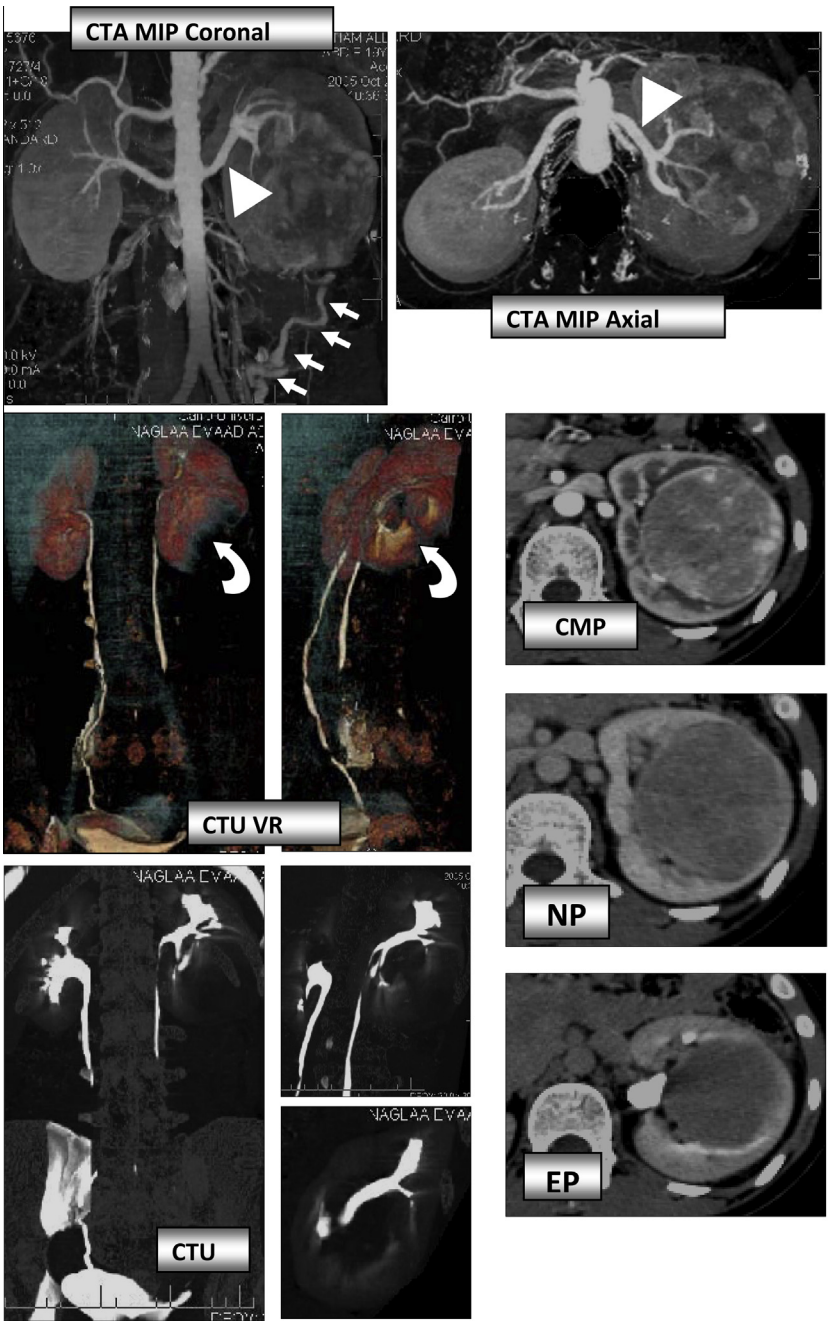

Fig. 5 A 19 year old female patient presented with left loin pain. US revealed left renal lower pole soft tissue mass. MDCT: Well defined large left middle and lower zonal soft tissue mass showing heterogeneous texture and measuring >7 cm in diameter. It shows intense enhancement in the CMP and rapid wash out in the following NP (HU is 148.4 in MP, 94.4 in NP and 88.7 in EP). No evidence of extension to perirenal fat or adrenals. Patent renal vein and IVC. No regional lymphadenopathy. No distant metastasis. CTA: Hypertrophied main renal artery and supplying segmental branches with early venous filling of the draining veins (arrows). CTU: Lower pole nephrogram defect (curved arrows) with compressed lower calyceal group, yet with no evidence of invasion. RCC.

enhancement was based on visual assessment and was therefore somewhat subjective.

Despite our small number of patient population we were able to predict certain particular patterns of enhancement in RCC and TCC cases. 39 RCC masses (regardless their pathological subtypes) showed intense enhancement in the CMP, rapid decrease of enhancement in the following NP denoting rapid wash out of contrast and final decrease of HU in the EP. A significant difference was detected between HU in CMP and EP in cases of RCC (P value = 0.0002) and difference between HU in NP and EP in cases of RCC (P value < 0.00001).

3 TCC lesions showed faint enhancement in the CMP, further increase of enhancement in the following NP and final decrease of HU in the EP. A significant difference was detected between HU in NP and EP in cases of TCC (P value = 0.03).

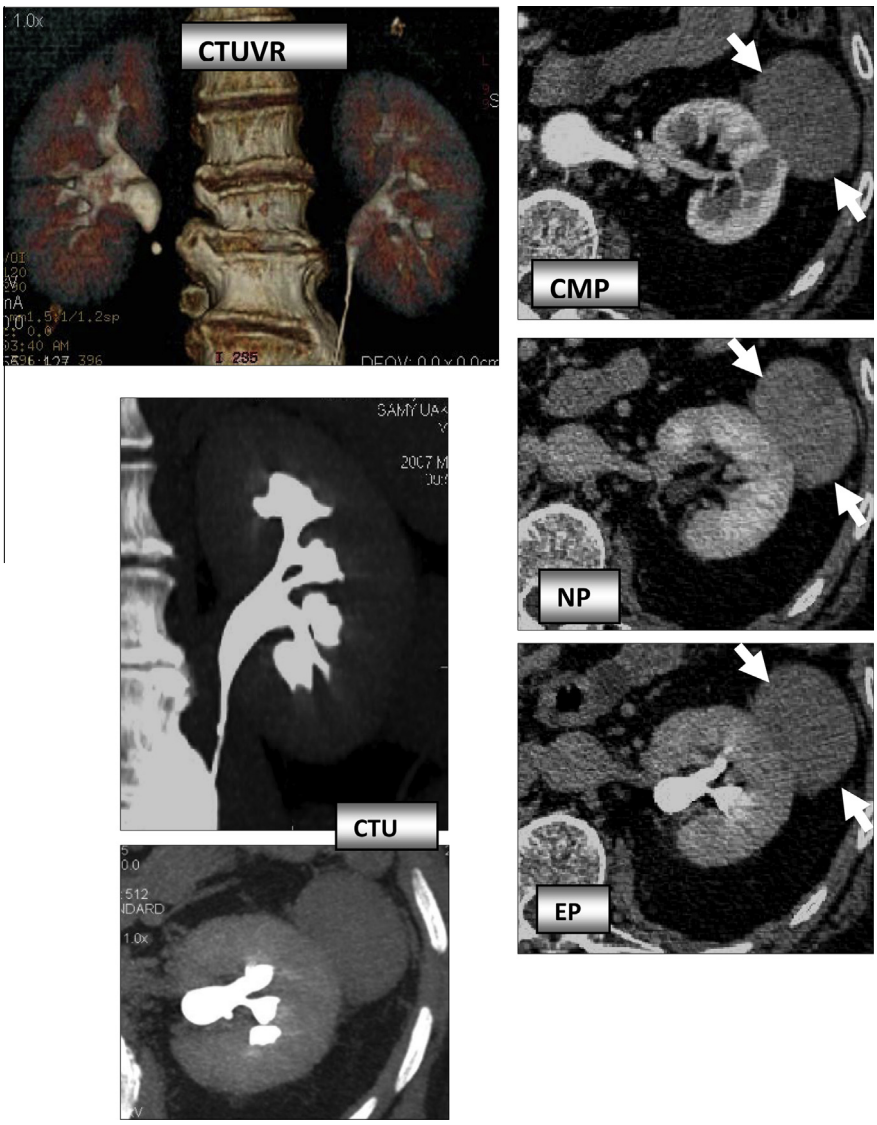

Fig. 6 MDCT: Well defined left renal middle zonal hypodense cortical lesion (arrows) measuring (> 4 cm in diameter). It shows small area of contact with the outer renal cortical surface. The mass shows evidence of enhancement throughout the phases (HU is 55.5 in MP, 83.1 in NP and 58.7 in EP). No adrenal masses. Patent renal vein and IVC. No regional lymphadenopathy. No distant metastasis. CTU: No abnormality detected. Diagnosis: Renal Cell Carcinoma (Papillary) T1b N0 M0.

Our study results showed that the presence of neovascularity was mildly associated with a more aggressive tumor which was rather an expected finding.

A limitation of our study was that the percentage of malignant lesions (88.5%) may have been slightly higher than that in the general population, since our institution is a tertiary referral center. However, even in the general population the incidence of malignant renal lesions is much higher than that of benign lesions.

In conclusion Multiphase CT has a major role in the diagnosis, characterization and staging of solid renal neoplastic masses. It also provides valuable data about the extent and spread of the mass, and fulfills information about vascular supply, venous thrombosis, excretory function and state of the pelvicalyceal system whether invaded, compressed or obstructed.

Conflict of interest

We have no conflict of interest to declare.

References

(1) Catalano C, Fraioli F, Laghi A, et al. High resolution multidetector CT in the preoperative evaluation of patients with renal cell carcinoma. AJR 2003;140:87–94.
(2) Ng Chaan S, Wood Christopher G, Silverman Paul M, Tannir Nizar M, et al. Renal cell carcinoma: diagnosis staging and surveillance. AJR 2008;191:1220–32.
(3) El-hefnawy AS, Mosbah A, El-Diasty T, et al. Accuracy of multidetector computed tomography (MDCT)in staging of renal cell carcinoma: anaslysis of risk factors for mis-staging and its impact on surgical intervension. World J Urol 2013;31(4):887–91.

(4) Goshima S, Kanematsu M, Nishibori H, Kondo H, Tsuge Y, Yokoyama R, et al. Multidetector row CT of the kidney: optimizing scan delays for bolus tracking techniques of arterial, corticomedullary, and nephrographic phases. Eur J Radiol 2007;63:420–6.
(5) Herts B, Coll D, Novick A, Obuchowski N, Linnell G, Wirth S, et al. Enhancement characteristics of papillary renal neoplasms revealed on triphasic helical CT of the kidneys. AJR 2002;178:367–72.
(6) Jinzaki M, Tanimoto A, Mukai M, et al. Double-phase helical CT of small renal parenchymal neoplasms: correlation with pathologic findings and tumor angiogenesis. J Comput Assist Tomogr 2000;24:835–42.
(7) Kim JK, Kim TK, Ahn HJ, Kim CS, Kim KR, Cho KS. Differentiation of subtypes of renal cell carcinoma on helical CT scans. AJR Am J Roentgenol 2002;178:1499–506.
(8) Rastogi N, Sahani DV, Blake MA, Ko DC, Peter RM. Evaluation of living renal donors: accuracy of three-dimensional 16-section CT. Radiology 2006;240:136–44.
(9) Ruppert-Kohlmayr AJ, Uggowitzer M, Meissnitzer T, Ruppert G. Differentiation of renal clear cell carcinoma and renal papillary carcinoma using quantitative CT enhancement parameters. AJR Am J Roentgenol 2004;183:1387–91.
(10) Russo P. Renal cell carcinoma: presentation, staging, and surgical treatment. Semin Oncol 2000;27:160–76.
(11) Sheir KZ, El-Azab M, Mosbah A, El-Baz M, Shaaban AA. Differentiation of renal cell carcinoma subtypes by multislice computerized tomography. J Urol 2005;174:451–5.
(12) Sheth S, Scatarige J, Horton K, Corl F, Fishman E. Current concepts in the diagnosis and management of renal cell carcinoma: role of multidetector CT and three-dimensional CT. Radiographics 2001;21:S237–54.
(13) Sheth S, Fishman E. Multi-detector row CT of the kidneys and urinary tract: techniques and applications in the diagnosis of benign diseases. RadioGraphics 2004;24:e20.
(14) Staehler G, Brkovic D. The role of radical surgery for renal cell carcinoma with extension into the vena cava. J Urol 2000;163:1671–5.
(15) Thrasher JB, Paulson DF. Prognostic factors in renal cancer. Urol Clin North Am 1993;20:247–61.
(16) Zagoria R. Imaging of small renal masses. AJR 2000;175:945–55.
(17) Zhang J, Lefkowitz RA, Ishill NM, Wang L, Moskowitz CS, Russo P, et al. Solid renal cortical tumors: differentiation with CT. Radiology 2007;244:494–504.
(18) Zhang J, Kang SK, Wang L, Touijer A, Hricak H. Distribution of renal tumor growth rates determined by using serial volumetric CT measurement. Radiology 2009;250:137–44.